Procedia Manufacturing

Volume 5, 2016, Pages 1283–1294

44th Proceedings of the North American Manufacturing Research Institution of SME http://www.sme.org/namrc

High Rate 3D Nanofabrication by AFM-Based Ultrasonic Vibration Assisted Nanomachining

Jia Deng, Jingyan Dong and Paul Cohen
North Carolina State University, Raleigh, U.S.
jdeng2@ncsu.edu, jdong@ncsu.edu,pcohen@ncsu.edu

Abstract
This paper introduces a high precision 3D nanofabrication approach using ultrasonic vibration assisted nanomachining using an AFM operating in constant height control mode. Nanostructures with 3D features were successfully fabricated on PMMA film with the feature height manipulated through controlling the absolute heights of z-scanner in AFM. Two methods were used to move the AFM tip to create desire features, vector mode and raster scan mode. Relatively simple features, such as stair-like nanostructure with five steps was successfully fabricated in vector mode. Complex nanostructure with discrete height levels and continuous changes were successfully fabricated in raster scan mode. By carefully selecting the machining parameters, the feature dimension and height can be precisely controlled with only small variation from the designed value. Moreover, this paper explores the capability of transferring 3D nanostructures from PMMA film onto silicon substrate. After calibrating the recipe of Reactive Ion Etching (RIE) process, 3D nanostructures are successfully transferred to silicon wafer with controllable selectivity between PMMA and silicon. The results of fabricating 3D structures on silicon substrates show promising potential of many applications, such as mold preparation in nanoimprint lithography.

Keywords: 3D nanomachining, Tip-based nanofabrication, Atomic Force Microscope (AFM), Ultrasonic *vibration* Assisted Nanomachining

1 Introduction

Nanotechnology as a cutting-edge engineering branch has provided significant impacts not only in fundamental sciences in physics, chemistry and biology, but also in applied engineering including electronic and mechanical devices. Many nanofabrication techniques have been developed, including nanomanipulation (Rubio-Sierra 2005), nanopatterning (Rosa 1998), nanomachining (Fang 2003), nanosurgery (Firtel 2004), nanodissection (Wen 2004), and tip-based nanomachining (Martín 2005, Martinez 2008, Piner 1999), which are mostly applied for 2D nanofabrication. Three dimensional (3D) nanofabrication approaches have attracted a lot of attention recently, motivated by many applications in various fields, such as optics, plasmonics, nanoelectromechanical systems (Fu 2011, Kettle 2008,

Selection and peer-review under responsibility of the Scientific Programme Committee of NAMRI/SME

doi:10.1016/j.promfg.2016.08.100

Keskinbora 2013, Yuan 2012). In order to satisfy the increasing needs of 3D nanostructures, a few 3D nanofabrication approaches have been developed recently. The typical approaches include grayscale e-beam lithography (EBL) (Yamazaki 2004), laser nanopatterning (Li 2011, Ali 2008), focused ion beam lithography (IBL) (Nellen 2006, Taniguchi 2006, and Villanueva 2006), UV nanoimprint lithography (Lee 2008), colloidal lithography (Yang 2006), anisotropic etching (Berenschot 2013), corner lithography (Berenschot 2008) and soft-lithographic techniques (Jeon 2004).

Among those 3D nanofabrication approaches, grayscale EBL is the most competitive one with the excellent resolution and process flexibility. The basic idea of grayscale EBL is to vary the writing dose of electron beam on resists based on pixel intensity. By changing the exposure dosage on resists at different locations, the exposed resist depth and the solubility of resists in the developer change accordingly. Stair-like 3D nanostructures have been fabricated through grayscale EBL (Hu 2003, Kim 2007, Lee 2008, Sure 2003, Totsu 2006). Despite the capability and flexibility of EBL, grayscale EBL has its own limitations due to the mechanism of the fabrication approach. The fabrication resolution is limited by the scattering effect of electrons in resists (Chang 1975, Owen 1983). Similar to focused ion beam lithography, the cost for EBL is relatively high due to the expensive EBL system.

Tip-based nanofabrication approaches have their unique advantages for 3D nanomachining. It is an approach with significantly lower cost compared with grayscale EBL when taking into account both the capital and maintenance costs. A combined AFM/precision-stage system has been developed to machine 3D nanostructures with complex geometries on Al samples by mechanical scratching (Yan 2010). An ultrasonic force regulated nanomachining approach was innovated for high rate nanomachining (Zhang 2012, Zhang 2013). A in plane circular xy-vibration and an ultrasonic vibration in z direction are utilized to improve the efficiency and performance of nanomachining processes. The xy-vibration is used as a means for controlling the width of trenches as well as increasing the material removal rate. The ultrasonic z-vibration is used to regulate the depth of machined features with the advantages of reduced normal force and lateral force (Zhang 2012, Zhang 2013). Trenches with widths ranging from tens to hundreds of nanometers and depths of a few to tens of nanometers can be created by a single machining path. Based on this high rate tip-based nanomachining approach, a 3D nanofabrication method was developed. A stair-like 3D nanostructure with 6 steps was fabricated layer-by-layer assisted by ultrasonic z-vibration under a given setpoint force. Convex and concave 3D circular features were fabricated by changing the setpoint force applied on sample surfaces (Deng 2015). Overlap rate in raster scan significantly affects the fidelity of final 3D nanostructures in this approach.

In this paper, an AFM-based precise 3D nanofabrication approach is developed using ultrasonic vibration assisted nanomachining in constant height control mode, in which absolute height values of the z-scanner are selected in AFM to regulate the feature depth in nanomachining. In the constant height control mode, the location of the cantilever tip is controlled directly when a rigid cantilever is used. During machining processes, the in-plane circular xy-vibration is utilized to control the virtual tool size and increase the machining speed. Two methods were used to move the AFM tip to create desire features, which are vector mode and raster scan mode. In vector mode, a stair-like 3D nanostructure with five steps is fabricated by moving the tip along the designed vector toolpath. In raster scan mode, the tip scans a predesigned bitmap image pixel-by-pixel with depth control by the grey scale value at each pixel. Nanostructures with discrete 3D levels of height were successfully fabricated. Moreover, 3D nanostructures with continuous changes in height were also fabricated in raster scan mode, including pyramids and cones. Discussions are made about the differences of fabrication processes under vector mode and raster scan mode. Finally, 3D nanostructures fabricated on PMMA surfaces were successfully transferred onto silicon surface by reactive ion etching (RIE). Resulting 3D nanostructures on silicon substrate indicate good feature transferability from PMMA to silicon.

2 Experimental Setup and Approach Design

2.1 Experimental Setup

The major components of the experimental system include a commercial AFM XE-70 from Park Systems Corporation, a customized nanovibrator, a signal access module from Park Systems, a data acquisition device from National Instruments Corporation (NI) and two signal amplifiers for two xy piezoelectric actuators respectively. The schematic of the experimental setup is illustrated in Figure 1 (a). The nanovibrator has an extruded pillar ($6 \times 6 \times 15$ mm) at the center of the platform. Two piezoelectric actuators are tightly mounted at the bottom of the pillar perpendicular to each other in order to provide high frequency in-plane circular xy-vibration. A detachable z piezoelectric actuator is glued on the top of the pillar to provide megahertz-level ultrasonic z-vibration. Samples to be machined are mounted on the top of the nanovibrator. The nanovibrator is screw tightened on the AFM scanner to provide ultrasonic vibration between the tip of AFM and samples.

In the system, two piezoelectric actuators are driven by sinusoid signals to generate sinusoid displacements with 90 degree phase difference in x and y directions. Therefore, a in plane circular xy-vibration is generated between the tip and the sample, which effectively forms a virtual tool for the machining processes, as shown in Figure 1 (b) and (c). With high frequency circular xy-vibration, only a thin slice of material is removed in one machining cycle, which greatly enhances the machining speed and reduces tip-sample interaction force. The radius of the virtual tool at a certain cutting depth is the sum of tip radius and the amplitude of the xy-vibration, which is around 15 nm if the vibrational command is 30mV. Here, the diameter of the virtual tool is controlled by the xy-vibration amplitude, which directly regulates the feature width that can be machined in one single machining path (Zhang 2012). The image of the new tip is shown in Figure 1 (f), which has a tip radius of 35nm. Ultrasonic z-vibration is used to reduce the friction force and regulate the feature depth during nanomachining processes. When z piezoelectric actuator drives samples to a frequency less than the resonant frequency of the cantilever (f < fr), the cantilever, contacting with the sample surface, follows the vibration of samples, as shown in Figure 1 (d). But when z-vibrational driving frequency is much higher than the resonant frequency of the cantilever (f >> fr), the cantilever dynamically 'freezes' due to its inertia and penetrates into sample surfaces, as shown in Figure 1 (e) (Zhang 2012, Zhang 2013). The feature depths are controlled by the amplitude of z-vibration. Besides the desired z-height change between tip and

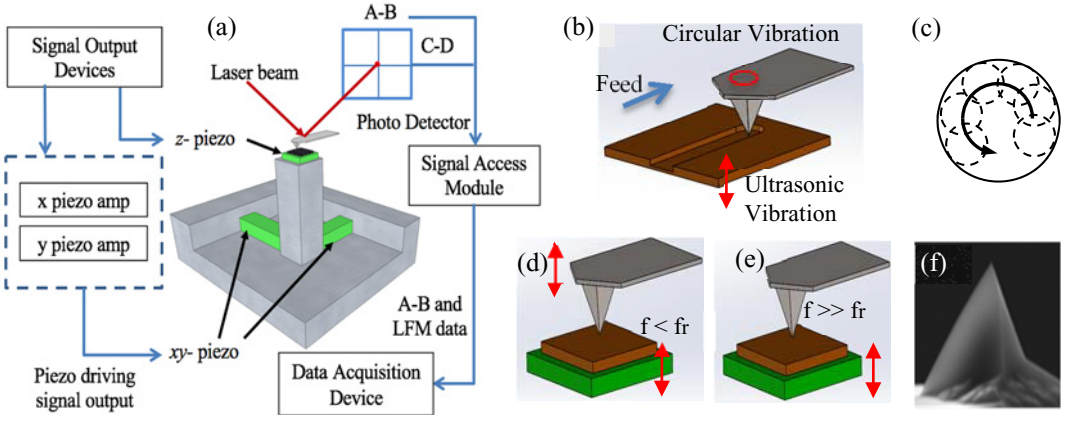

Figure 1. (a) Schematic illustration of experimental setup. (b) Schematic illustration of nanomachining assisted by vibration. (c) Virtual tool when tip is vibrated with a xy circular path. (d) Tip-sample interaction with z-vibration in low frequency. Tip vibrates with z-piezo. (e) Tip-sample interaction with z-vibration in ultrasonic frequency. Tip does not vibrate with z-piezo, "freezing" at the current location. (f) SEM image of an AFM tip

sample from z piezoelectric actuator, lateral displacements of pillar top from xy-vibration also leads to changes in height. However, the value of the changes from ANSYS simulation is only around 10 nm across 3 mm lateral motion. Thus, changes of height in z-direction caused by xy-vibration are negligible since lateral dimensions of 3D nanostructures are often in the level of a few micrometers. Setpoint forces between the AFM tip and sample surfaces are measured by the optical system and photo detector, and are controlled through the feedback control system in the AFM.

In our experiments, 3D nanostructures were first created on PMMA film, which is a commonly used resist for photolithography and EBL. PMMA (950 PMMA A4 from Microchem, 4% dilution in anisole) was spin coated on cleaned silicon wafers at 4000 RPM for 40 s by a Headway Spinner. Then silicon wafers were baked at 180 °C for 90s. The final PMMA thickness is around 200 nm. Tips used in experiments are silicon with diamond like carbon (DLC) coatings. Dimensions of cantilevers are $225 \times 387 \times 7$ μm. The nominal stiffness and resonant frequency are 48 N/m and 190 KHz respectively. According to our previous tip wear experiments, tip radius only increases slightly from 35nm to 50nm after fabricating trenches with total length of 1500um on PMMA (Zhang 2013). Thus the tip wear after the nanomachining process with a few patterns is negligible. In this study, the same cantilever that is used in the machining process is also used to image the features directly after the machining process.

2.2 Process Design for 3D Nanofabrication

Our previous research has demonstrated that 3D nanostructures can be fabricated using ultrasonic vibration assisted nanomachining (Deng 2015) with feature depth controlled by setpoint force. Ideally, setpoint force can be reliably used to control the feature depth, even for non-flat surfaces. However, it is very difficult for the control system to keep the required setpoint force with fast-change command and disturbance. Since the required setpoint force is reduced significantly with the help of z-vibration, a disturbance will have a relatively large influence on the process. Moreover, with this depth control approach, the overlap percentage between neighboring features significantly affects the final 3D nanostructures. If the overlap percentage is too large (>60%), the newly machined features are overlapped a lot with previously fabricated areas. The overlapped area can be machined two or more times under the same setpoint force, which as a result, makes depth control very difficult.

In this paper, we investigate the capability of constant height mode for AFM-based 3D nanofabrication. In the constant height mode, the absolute z-location of the cantilever is directly specified by the user and controlled by the z-scanner. If the cantilever is rigid enough, the location of the cantilever can be selected directly for machining features with designed depth. In the nanolithography software provided by Park Systems, the cantilever heights can be set for features designed in vectors or bitmap images. Vectors and bitmap images represent two approaches to define the feature geometry in xy-plane, implemented in two lithography-working modes: vector mode and raster scan modes, as shown in Figure 2.

In vector mode, six basic shapes can be chosen and combined to design the patterns to be machined. These basic shapes are point, line, rectangle, ellipse, polygon and polyline. In the lithographic software,

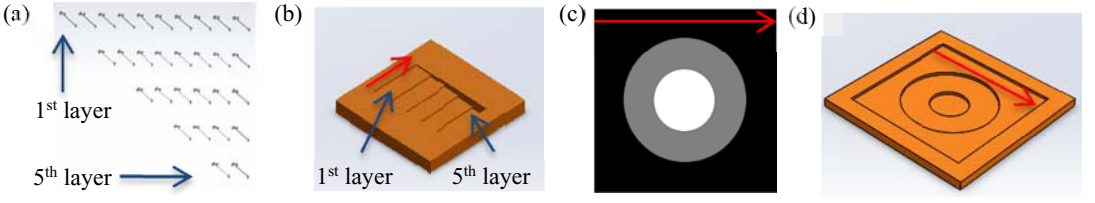

Figure 2. (a) Schematic of vector mode with an example of five layers 3D nanostructure. (b) Feature after fabrication in vector mode. Red line shows the machining direction. (c) Schematic of raster scan mode with 3D nanostructure of three concave layers represented by grey scale bitmap image. (d) Design feature in raster scan mode with depth represented by the grey scale. Red line shows the scan direction.

vector and features can be designed precisely with sub-nanometer resolution. The tip follows the vector-based trajectory (i.e. toolpath) one by one according to the specified sequence until all of them are machined. The z-height of the feature is controlled by setting two values for each vector, the starting point height and ending point height. If the height for the start point and the end point is different, the tip height changes continuously from the starting point to the end. Figure 2 (a) and (b) give an example that uses vector mode to produce 3D nanostructure with 5 stairs (Figure 2b). Five layers of vectors are designed as the toolpath to machine the five stairs (Figure 2a).

In raster scan mode, the features are designed as a bitmap image. The tip scans the image pixel-by pixel from the left to the right and from the top to the bottom. After finishing one line, the tip lifts up and moves to the second line below it. The entire machining process ends at the bottom-right corner. The tip trajectories are parallel lines with directions from the left to the right. The schematic of the machining process is illustrated in Figure 2 (c). Complex structures can be designed much easier than in vector mode. The grey scale of the bitmap image corresponds to height values. The brightest color and the darkest color in the bitmap images represent the maximum and minimum height values respectively, and the height values are linearly interpolated by the gray scale value. By designing proper grayscale in bitmap images, heights of the feature can be precisely specified. Figure 2 (c) and (d) show a desired 3D structure and the corresponding bitmap image for machining the same structure. In raster scan mode, pixels in the bitmap image represent the resolution of the designed feature for machining processes. The number of pixels in the column is the number of traces the AFM tip scans laterally, which determines the overlap rate between two adjacent machining paths when the virtual tool size is given. The pixels in rows determine the in-plane feature resolution where the tip height changes.

The overall nanofabrication procedure on PMMA film includes six steps as follows. 1) Image an area under tapping mode; 2) Design patterns or loading bitmap images for the structure to be machined; 3) Select constant height control mode for AFM in nanolithography software; 4) Apply ultrasonic vibration assisted nanomachining processes for the designed patterns; 5) Clean the sample with ultrasonic agitation after machining to remove debris; and 6) Reimage the 3D nanostructures after a washing process. The washing process is necessary in order to remove the debris from the machining process and achieve clear and accurate results. The washing procedures are as follows: 1) Wash the sample with ultrasonic agitation in 30% wt aqueous solution of acetone for 2 minutes, 2) Flux the sample with DI water for 10s, and 3) Flux the sample with IPA solution and bake at 90 °C for 2 minutes. The concentration of the aqueous solution of acetone is suitable for removing debris while not damaging machined features. After fabricating 3D nanostructures on PMMA film, RIE process is utilized to transfer 3D nanostructures from PMMA surfaces onto a silicon substrate. Semigroup RIE system is used in our experiments to obtain 3D nanostructure on silicon substrate.

3 Experimental Results and Discussion

We applied ultrasonic vibration assisted nanomachining with constant height control mode to evaluate the capability in the fabrication of 3D nanostructures. By directly controlling the tip height, 3D nanostructures are successfully fabricated with precisely controlled feature dimensions. In this study, both the vector mode and raster scan models are applied for 3D nanostructure fabrication. In vector mode, a stair-like 3D nanostructure with five height levels are fabricated. In raster scan mode, various complex 3D nanostructures are fabricated, which include features with both discrete height levels and continuous height changes. The fabrication results demonstrate the strong capability of ultrasonic vibration assisted nanomachining in 3D nanofabrication.

In our experiment, a stair-like 3D nanostructure with five steps is machined in vector mode, which has the height of each level of 20 nm. Layer by layer technique is applied to fabricate at each height level. The fabrication process starts with the first layer, in which the z scanner of AFM is moved downwards 35 nm from the PMMA surface. An extra 15 nm depth is used for the first layer to

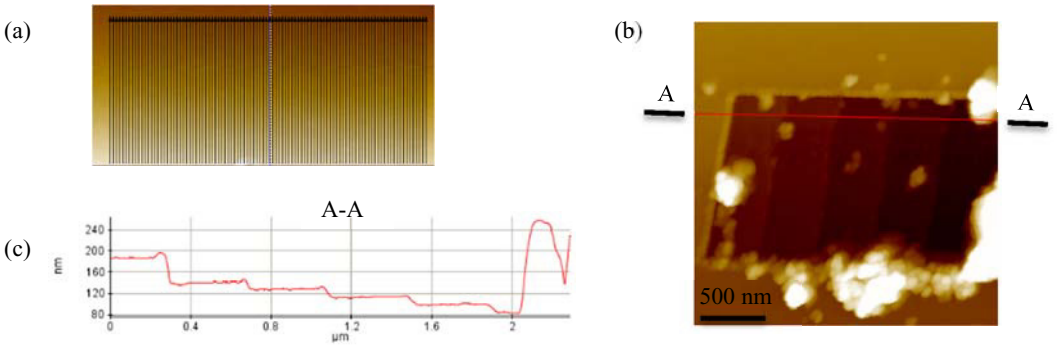

Figure 3. (a) Vectors designed in lithographic software. (b) A stair-like 3D nanostructure with five steps after nanomachining. (c) Cross sectional profile of the five steps.

compensate for any surface non-flatness. Following the first layer, the rest of the layers are machined one by one in sequence with tip height reduced 20 nm for each subsequent layer. The schematic of the design is illustrated in Figure 3 (a). For the first layer, 100 parallel lines are designed in order to cover the entire machining area with 2 μm in length. Distances between every two adjacent lines are designed as 20 nm. The selection of the gap between two lines depends on the size of the virtual tool and the overlap percentage that can provide good machining performance. When the overlap rate is too large, more lines are needed to machine the same area, which increases the machining time and tip wear. When the overlap rate is too small, machined surface quality may not be satisfactory. For the five layers, there are 100, 80, 60, 40, 20 lines from the top layer to the bottom feature.

After the machining and cleaning processes, the five level stair nanostructure was successfully fabricated, as shown in Figure 3 (b). Heights from the top to the bottom layer are 45 nm, 15 nm, 16 nm, 15 nm and 15 nm respectively, as shown in Figure 3 (c). The first layer can be treated as an initial calibrating layer to remove the non-flatness and non-parallelism between the sample surface and xy-plane of the AFM. For the remaining layers, the resulting height is 5 nm less than the designed height. The difference in height comes from the non-rigid cantilever. Since the spring constant of the cantilever is not infinitely large, the tip-sample interaction deflects the cantilever from the design displacement from the z-scanner. As the result, the actual feature depth is a little less than the designed height. The height difference between the actual value and the designing value can be compensated for by selecting a larger depth in design. The cross sectional profile in Figure 3 (c) shows uniform and flat five stairs with average surface roughness of 0.5 nm. The walls between two steps are not perfectly perpendicular to the steps because of round shape of the tip and the virtual tool, which leads to a slightly sloped wall between two layers.

To evaluate the 3D fabrication capability in raster scan mode, we designed a 3D nanostructure with two deep circles and a shallow square, as shown by bitmap images in Figure 4(b) and (d). The schematic of fabrication process is illustrated in Figure 2 (b). The tip machines the area from the top-left corner to the right and gradually scans down as process proceeds. Wherever there is a color change, the height of the tip changes accordingly. Depths designed for the layers with black, 50% gray, and white color are 15 nm, 45 nm and 75 nm respectively. Since the lateral dimensions of the pocket are 1.5 μm and the size for each pixel is selected 20 nm, the bitmap image has 75 pixels in each row and column. Similar to the vector scan mode, the pixel value needs to be selected carefully to achieve the good machining performance with minimum cycle time. The scanning speed is set as 0.5 μm/s, which is the same as the machining speed in vector mode.

After machining and washing away the debris processes, Three-layer 3D nanostructures were successfully fabricated and imaged, as shown in Figure 4 (a) and (c). Actual depths for the layers with black, 50% gray, white color are 12 nm, 42 nm and 74 nm respectively. Actual heights are only around

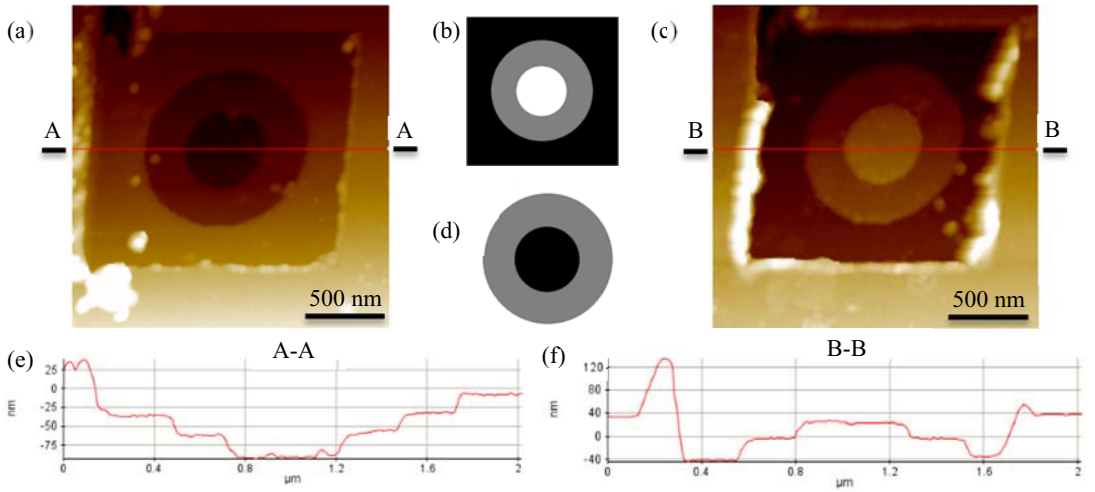

Figure 4. (a) Three-layers nanostructure with two circular cavities. (b) Bitmap image designed for the three-layer 3D nanostructure. (c) Three-layer nanostructure with two circular protrusions. (d) Bitmap image designed for 3D nanostructure with two convex circles. (e) Cross sectional profile of 3D nanostructure with two circular cavities. (f) Cross sectional profile of nanostructure with two circular protrusions.

2-3 nm less than the designed heights. The nanomachining approach reproduce the 3D nanostructrues from the bitmap image with very good fidelity.

Comapring the vector mode and the raster scan mode in 3D nanomachining, the vector mode is more efficient for sparse pattern fabrication, and the raster scan mode is capable for the fabrication of very complicated structures. Users can conveniently design the trajectory (i.e. toolpath) of the tip under the vector mode and arrange vectors together to get sparse nanostructures without scanning through allareas. However, it is much easier to design and fabricate complex 3D nanostructures using bitmap images in raster scan mode. For example, the stair-like structure in Figure 3 can be conveniently fabricated using the vector mode, but it is very difficult for users to design and manually arrange vectors in order to

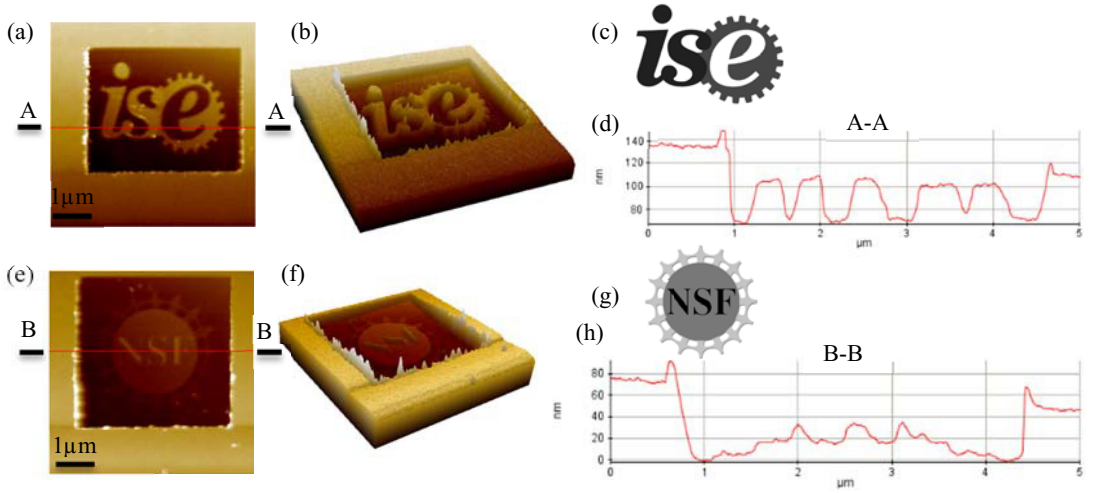

Figure 5. (a) 3D nanostructure of letters “ise”. (b) 3D view of “ise”. (c) Bitmap images of “ise”. (d) Cross sectional profile of “ise” letters. (e) 3D nanostructure of “NSF” logo. (f) 3D view of “NSF” logo. (g) Bitmap image of “NSF” logo. (h) Cross sectional profile of “NSF” logo.

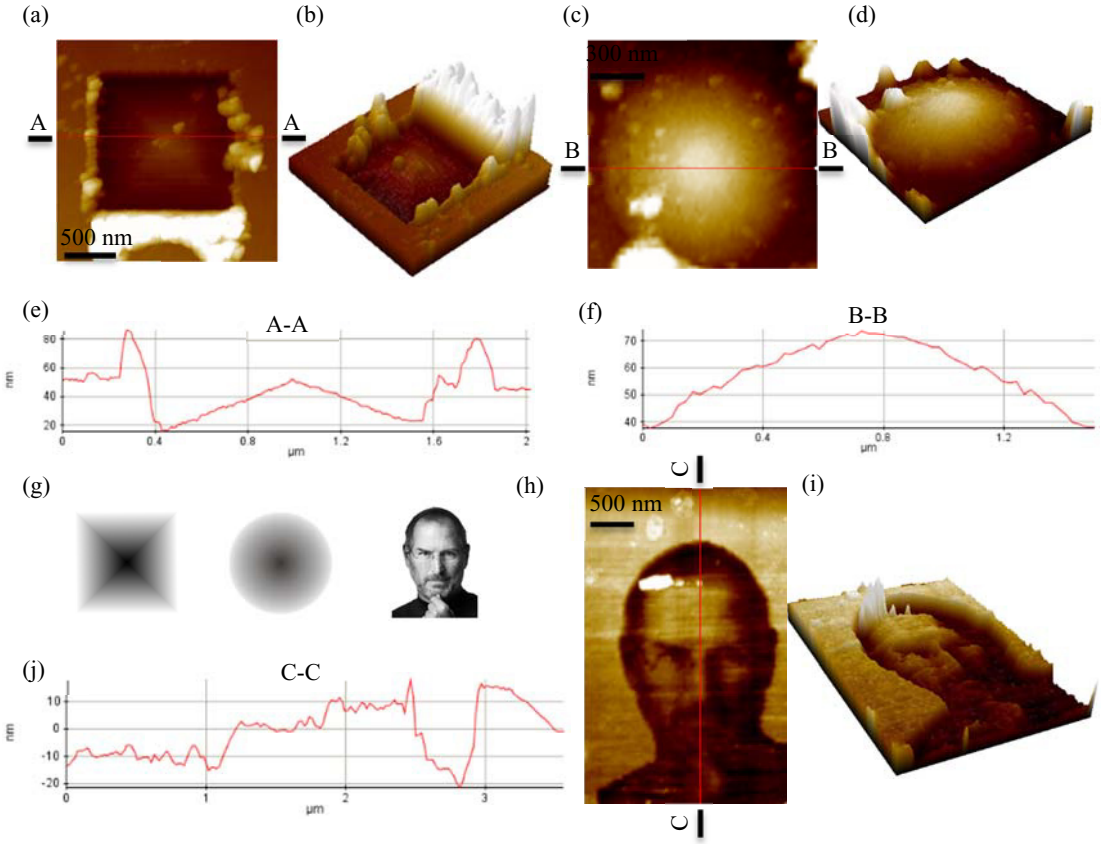

Figure 6. (a) Fabricated pyramid nanostructure and its (b) 3D view. (c) Fabricated cone nanostructure and its (d) 3D view. (e) Cross sectional profile of the pyramid. (f) Cross sectional profile of the cone. (g) Bitmap images of pyramid, cone and Jobs' profile. (h) 3D nanostructure, and (i) 3D view of Jobs' profile.

create a circle. Another concern between two modes is that the spring constant of the cantilever is not the same when machining in different direction. However, with the help of xy-vibration, cantilever with nominal stiffness of 48N/m is stiff enough in raster scan mode. As shown in Figure 4, the depths achieved in raster scan mode are very close to the designing depths. Therefore, we use raster scan mode to further investigate the capabilities of the 3D nanofabrication approach for complex structure fabrication.

Complex nanostructures represented by bitmap images as shown in Figure 5 were used to investigate the fabrication ability of nanomachining approach. Bitmap images of the "ise" and "NSF" logos were designed with different gray scale, as shown in Figure 5 (c) and (g). In the "ise" logo, the letter "i" and "s" are black, "e" is 73% gray. Height from bottom to "is" is designed as 35 nm and height difference between "is" and "e" is designed as $35\times0.27=9.45$ nm. The overall size of "ise" logo is 3.6×3 μm. In the logo of "NSF", three letters "NSF" are black, the circle under NSF are 67% gray and the outside ring is 33% gray. Height from bottom to "NSF" is designed as 45 nm. Height from "NSF" to the circle is designed as 15 nm. Height from the circle to the outside ring is designed as 15 nm. The overall size of "NSF" is 3.6×3.6 μm. Density of designing pixels in all three nanostructures are 80/μm.

The nanostructures from the 3D nanomachining successfully replicate the designed bitmap images onto PMMA film. In the logo of "ise", high-resolution features, such as the gear teeth with width of around 200 nm were successfully produced. Height of "is" is 39.5 nm and height difference between "is" and "e" is 6.5 nm. In the logo of "NSF", heights of the outside ring, the circle and the "NSF" are

around 9 nm, 20 nm and 34 nm respectively. 3D views of the two logos were shown in Figure 5 (b) and (f). Three results demonstrate the capability of fabricating the 3D nanostructure with complex geometry using the nanomachining approach.

Moreover, nanostructures with continuous height changes are designed and fabricated by nanomachining in raster scan mode. Results of pyramid, cone and a Steve Jobs' profile are shown in Figure 6 (a), (c) and (h) respectively. The 3D view of these structures were shown in Figure 6 (b), (d) and (i) respectively. Cross sectional profile of them are shown in figure 6 (e), (f) and (j) respectively. The total designed heights for these structures are all 40 nm from the bottom to top. Resulting heights are 35 nm, 36 nm and 36 nm respectively. Shapes and dimensions were fabricated in close correspondence to the designed values. All the results strongly demonstrate the capability of the nanomachining approach in constant height control mode for 3D nanostructures fabrication.

4 Transferring 3D Nanostructures to Silicon

The 3D nanostructures fabricated on PMMA surfaces can be further transferred onto silicon substrates for a broad range of applications, such as nanomolds for nanoimprint lithography. We developed an RIE (Reactive Ion Etching) recipe of using SF_6 and O_2 to etch the PMMA and silicon substrates. The height difference in PMMA film will be transferred to the underneath silicon substrate to produce 3D structures on silicon. The equipment we used is a Semigroup Reactive Ion Etcher. The plasma power of 24 W, flow rate of SF_6 and O_2 of 18 sccm and 5 sccm respectively were selected for the etching process. Pressure in the chamber is set to be 40 mtorr. The etching rate for PMMA and Si were identified to be around 0.7 nm/s and 1.1 nm/s respectively. The selectivity of PMMA to silicon is about 1.5, indicating that when 1 nm PMMA is etched away, 1.5 nm silicon is etched at the same time. After 3 minutes etching, the PMMA film was completely etched, and 3D nanostructures can be fully transferred on the silicon surface.

We performed RIE etching experiments using a three-step stair-like 3D nanostructure on PMMA. Before RIE etching, depths each step were 9nm, 29nm and 30nm respectively, as shown in Figure 7 (a)

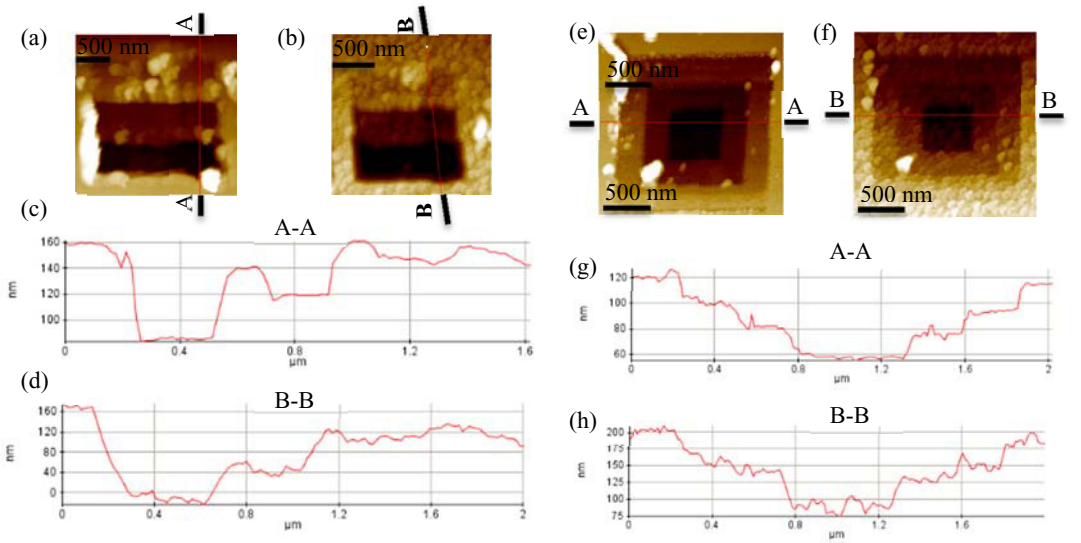

Figure 7. (a) A three-step stair nanostructure on PMMA film. (b) The stair nanostructures on silicon substrate after RIE. (c,d) Cross sectional profile of the stair structure on PMMA and silicon. (e) Nanostructures with three levels of square cavities on PMMA. (f) Nanostructures with three levels of square cavities on silicon after RIE. (g) Cross sectional profile of three levels of square cavities on PMMA and silicon.

and (c). After RIE etching, the stair-like 3D nanostructures with three steps was successfully transferred onto the silicon substrate, as shown in Figure 7 (b). The entire structure on silicon is clean and clear. PMMA debris residue that was not washed away during cleaning process was etched out during the RIE process. Depths of each layer on silicon are around 20 nm, 58nm and 64nm, as shown in Figure 7 (d). The surface roughness is around 7nm. We also tried to transfer relatively complex nanostructures with discrete height levels to silicon substrate. A three-level square cavity structure was fabricated using our nanomachining approach and then was transferred onto the silicon surfaces by RIE etching, as shown in Figure 7 (e) and (f). Height differences are about 20nm for each designed levels. Results on silicon show good fidelity of transferring 3D nanostructures from PMMA surfaces to silicon surfaces.

5 Conclusions

In this paper, we introduce a high rate 3D nanofabrication approach by ultrasonic vibration assisted nanomachining using an AFM operating in constant height control mode. By directly controlling the absolute heights of z-scanner in AFM, nanostructures with 3D features were successfully fabricated on PMMA film. We studied two methods to design features to be machined, which are vector mode and raster scan mode. Relatively simple features, such as stair-like nanostructure with five steps was successfully fabricated in vector mode. Complex nanostructure with discrete and continuous height changes were successfully fabricated in raster scan mode from bitmap images. By carefully selecting the machining parameters, the feature lateral dimension and height can be precisely controlled with only small variation from the designed value. Moreover, this paper explores the capability of transferring 3D nanostructures from PMMA film onto silicon substrate through Reactive Ion Etching (RIE). After calibrating the recipe of RIE process, 3D nanostructures were successfully transferred to silicon wafer with controllable selectivity between PMMA and silicon. The results of fabricating 3D structures on silicon substrates show promising potential of many applications, such as mold preparation in nanoimprint lithography.

Acknowledgement

This work was supported in part by the National Science Foundation under Grant Award NSF CMMI-1233176.

References

Ali M, Wagner T, Shakoor M, Molian PA. Review of laser nanomachining. *Journal of Laser Applications* 2008; 20(3): 169-184.

Berenschot EJ, Jansen HV, Tas NR. Fabrication of 3D fractal structures using nanoscale anisotropic etching of single crystalline silicon. *Journal of Micromechanics and Microengineering* 2013; 23(5): 055024.

Berenschot EJ, Tas NR, Jansen HV, Elwenspoek M. 3D-nanomachining using corner lithography. In *Proceeding of 3rd IEEE International Conference on Nano/Micro Engineered and Molecular Systems*, 2008, pp. 729-732.

Chang, T. H. P. "Proximity effect in electron-beam lithography." *Journal of Vacuum Science & Technology* 12.6 (1975): 1271-1275.

Fang TH and Chang WJ. Effects of AFM-based nanomachining process on aluminum surface. *Journal of Physics and chemistry of Solids* 2003; 64(6): 913-918.

Deng J, Zhang L, Dong J, Cohen PH, AFM-based 3D Nanofabrication Using Ultrasonic Vibration Assisted Nanomachining, *Procedia Manufacturing*, Volume 1, (2015), 584-592.

Firtel M, Henderson G, Sokolov I. Nanosurgery: observation of peptidoglycan strands in Lactobacillus helveticus cell walls. *Ultramicroscopy* 2004; 101(2): 105-109.

Fu, Yongqi, Fengzhou Fang, and Zongwei Xu. *Nanofabrication and characterization of plasmonic structures*. INTECH Open Access Publisher, 2011.

Hu, Fei, and Soo-Young Lee. "Dose control for fabrication of grayscale structures using a single step electron-beam lithographic process." *Journal of Vacuum Science & Technology B* 21.6 (2003): 2672-2679.

Jeon, Seokwoo, et al. "Three-Dimensional Nanofabrication with Rubber Stamps and Conformable Photomasks." *Advanced Materials* 16.15 (2004): 1369-1373.

Kettle, J., et al. "Overcoming material challenges for replication of "motheye lenses" using step and flash imprint lithography for optoelectronic applications." *Journal of Vacuum Science & Technology B* 26.5 (2008): 1794-1799.

Kim, J., D. C. Joy, and S-Y. Lee. "Controlling resist thickness and etch depth for fabrication of 3D structures in electron-beam grayscale lithography." *Microelectronic Engineering* 84.12 (2007): 2859-2864.

Lee KS, Kim RH, Yang DY, Park SH. Advances in 3D nano/microfabrication using two-photon initiated polymerization. *Progress in Polymer Science* 2008; 33(6): 631-681.

Lee, S-Y., and K. Anbumony. "Accurate control of remaining resist depth for nanoscale three-dimensional structures in electron-beam grayscale lithography." *Journal of Vacuum Science & Technology B* 25.6 (2007): 2008-2012

Li L, Hong M, Schmidt M, Zhong M, Malshe A, Huis in'tVeld B, Kovalenko V. Laser nano-manufacturing–state of the art and challenges. *CIRP Annals-Manufacturing Technology* 2011; 60(2): 735-755.

Martinez J, Martínez RV, Garcia R. Silicon nanowire transistors with a channel width of 4 nm fabricated by atomic force microscope nanolithography. *Nano Letters* 2008; 8(11):3636-3639.

Martín C, Rius G, Borrisé X, Pérez-Murano F. Nanolithography on thin layers of PMMA using atomic force microscopy. *Nanotechnology* 2005; 16(8): 1016.

Murray, W. Andrew, and William L. Barnes. "Plasmonic materials."*Advanced Materials* 19.22 (2007): 3771-3782.

Nellen PM, Callegari V, Brönnimann R. FIB-milling of photonic structures and sputtering simulation. *Microelectronic Engineering* 2006; 83(4): 1805-1808.

Owen, Geraint, and Paul Rissman. "Proximity effect correction for electron beam lithography by equalization of background dose." *Journal of Applied Physics* 54.6 (1983): 3573-3581.

Piner RD, Zhu J, Xu F, Hong S, & Mirkin CA. "Dip-pen" nanolithography. *Science* 1999; 283(5402): 661-663.

Rosa JC, Wendel M, Lorenz H, Kotthaus JP, Thomas M, Kroemer H. Direct patterning of surface quantum wells with an atomic force microscope. *Applied Physics Letters* 1998; 73(18): 2684-2686.

Rubio-Sierra FJ, Heckl WM, Stark RW. Nanomanipulation by atomic force microscopy. *Advanced Engineering Materials* 2005; 7(4): 193-196.

Sure A, Dillon T, Murakowski J, Lin C, Pustai D, Prather D. "Fabrication and characterization of three-dimensional silicon tapers." *Optics Express* 11.26 (2003): 3555-3561.

Taniguchi, Jun, et al. "Rapid and three-dimensional nanoimprint template fabrication technology using focused ion beam lithography." *Microelectronic Engineering* 83.4 (2006): 940-943.

Totsu, Kentaro, et al. "Fabrication of three-dimensional microstructure using maskless gray-scale lithography." *Sensors and Actuators A: Physical* 130 (2006): 387-392.

Villanueva G, Plaza JA, Sánchez-Amores A, Bausells J, Martínez E, Samitier J, Errachid A. "Deep reactive ion etching and focused ion beam combination for nanotip fabrication." *Materials Science and Engineering: C*26.2 (2006): 164-168.

Wen CK, Goh MC. AFM nanodissection reveals internal structural details of single collagen fibrils. *Nano Letters* 2004; 4(1): 129-132.

Yamazaki K, Yamaguchi T, Namatsu H. Three-dimensional nanofabrication with 10-nm resolution. *Japanese Journal of Applied Physics* 2004; 43(8B): L1111.

Yang SM, Jang SG, Choi DG, Kim S, Yu HK. Nanomachining by colloidal lithography. *Small* 2006; 2(4): 458-475.

Yan Y, Hu Z, Zhao X, Sun T, Dong S, Li X. "Top-Down Nanomechanical Machining of Three-Dimensional Nanostructures by Atomic Force Microscopy." *Small* 6.6 (2010): 724-728.

Yuan, Wu, Fei Wang, and Ole Bang. "Optical fiber sensors fabricated by the focused ion beam technique." *OFS2012 22nd International Conference on Optical Fiber Sensor*. International Society for Optics and Photonics, 2012.

Zhang L, Dong J. High-rate tunable ultrasonic force regulated nanomachining lithography with an atomic force microscope. *Nanotechnology* 2012; 23(8): 085303.

Zhang L, Dong J, Cohen PH. Material-insensitive feature depth control and machining force reduction by ultrasonic vibration in AFM-based nanomachining. *IEEE Transactions on Nanotechnology* 2013; 12(5): 743-750.